Broadband frequency mode entanglement in waveguided parametric downconversion

Andreas Eckstein* and Christine Silberhorn

Max Planck Research Group, Günther-Scharowsky-Strasse 1, 91054 Erlangen, Germany
*Corresponding author: aeckstein@optik.uni-erlangen.de

We report the observation of beatings of the coincidence event rate in a Hong–Ou–Mandel interference (HOMI) between signal and idler photons from a parametric downconversion (PDC) process inside a multimode KTP waveguide. As an explanation we introduce biphotonic states entangled in their broadband frequency modes generated by waveguide mode triples and propose a suitable entanglement detection scheme. © 2008 Optical Society of America

OCIS codes: 270.4180, 130.2790.

Waveguided parametric downconversion (PDC) is a promising approach to realize photon pair sources for applications in quantum communication [1] or quantum imaging [2]. The mode confinement of the waveguide allows for a significant increase of the source brightness in comparison to bulk crystal setups [3–5]. In addition, owing to the guiding structure, a PDC process in a nonlinear waveguide will produce photon pairs in distinct spatial modes [6], which contrasts to the continuous distributions defined by phase matching inside bulk crystals. While for bulk crystals the photon pairs are generally correlated in their transverse momenta, the waveguide also enforces decorrelation of the spatial signal and idler modes. However, in general a PDC process introduces an interrelation between the spatial properties of the pump and the spectral distributions of signal and idler photons [6,7] as well. We expect to find a similar behavior for the waveguided case.

The Hong–Ou–Mandel interference (HOMI) [8] is widely used to probe the spatial-spectral structure of single photon pairs. It measures the exchange parity of a two-photon state by detecting a coincidence probability in dependence of the overlap of both input modes [9] and thus offers information on the correlations of a biphotonic state. This has been applied to the polarization [10], temporal [11], or spatial [12] degree of freedom; deviation from the classic dip signature hints at entanglement.

In this Letter, we employ waveguided PDC and study the spectral structure of its resulting biphotonic state, which is strongly affected by the discrete spatial modes of the pump. We introduce entanglement of discrete broadband frequency modes and for the first time (to our knowledge) provide a characterization of states with disjoint biphoton spectral intensities as illustrated in Fig. 1(b). For such states, a Hong–Ou–Mandel (HOM) experiment results in beatings in the coincidence event detection, which have been reported for settings using frequency postselection [13–15] or active phase manipulation [16]. We on the other hand demonstrate a generation of these states inside a waveguide without additional manipulation and use the signature of an HOM experiment as a witness of entanglement, analogous to the the well known Bell-state analyzer [10,17].

Broadband photon creation $\hat{A}_f^\dagger$ operators may be defined by monochromatic creation operators $\hat{a}^\dagger(\omega)$ as

$$\hat{A}_f^\dagger = \int \mathrm{d}\omega f(\omega)\hat{a}^\dagger(\omega), \tag{1}$$

with the function $f(\omega)$ specifying the spectral amplitude of the photon. Any amplitude function $f(\omega)$ can be expanded into a basis set of orthogonal functions such that the single photon state may be decomposed into a superposition of broadband single-photon states with orthonormal amplitude functions $|\psi\rangle = \hat{A}_f^\dagger|0\rangle = \Sigma_{i=0}^\infty c_i \hat{A}_{u_i}^\dagger|0\rangle$. Let $u_i(\omega)$ denote the Hermite functions and $\hat{A}_{u_i}^\dagger$ be a broadband mode creation operator as defined in Eq. (1) with a Hermite function as the amplitude.

Let us now construct a maximally entangled two-photon state using the $u_i(\omega)$ as a basis of frequency modes

$$|\psi^-\rangle = \frac{1}{\sqrt{2}}[\hat{A}_{u_0}^\dagger \hat{B}_{u_1}^\dagger - \hat{A}_{u_1}^\dagger \hat{B}_{u_0}^\dagger]|0\rangle, \tag{2}$$

with A and B signifying signal and idler modes, respectively. The structure of $|\psi^-\rangle$ is formally analogous to the polarization entangled singlet Bell-state, where the Hermite functions $u_0(\omega)$ and $u_1(\omega)$ are replaced by the horizontal and vertical polarizations. The resulting joint spectral amplitudes with contributions $u_i(\omega_i)$ and $u_j(\omega_s)$ for two-party systems are illustrated in Figs. 1(a) and 1(b). A Bell-state analyzer [17] allows one to identify a polarization singlet state by an HOM-type experiment by measuring quantum interference at a balanced beam splitter between the
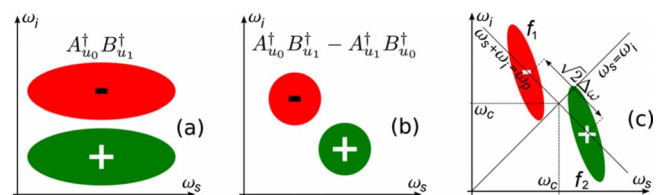
Fig. 1.   (Color online) (a),(b) Shape of joint spectral amplitudes for combinations of lowest-order Hermite functions and (c) shape of superimposed PDC processes.

© 2008 Optical Society of America

modes A and B in dependence of their polarization overlap [10]. Here only an entangled singlet state exhibits the signature of photon antibunching, which is proof of entanglement.

In the following we will show that an analogous criterion can be constructed for broadband entangled modes in a standard HOM experiment. Consider a standard HOM experiment for a biphotonic state with joint spectral amplitude $f(\omega_s, \omega_i)$. The two photons are fed into a balanced beam splitter with varying time delay τ, and the outputs are monitored by binary photon detectors. The probability to detect a coincidence event from both detectors for each arriving photon pair is then given by

$$p(\tau) = \frac{1}{2} - \frac{1}{2} \frac{\mathrm{Re}\left[\iint \mathrm{d}\omega_s \mathrm{d}\omega_i f^*(\omega_s, \omega_i) f(\omega_i, \omega_s) e^{-\imath \tau(\omega_s - \omega_i)} \right]}{\iint \mathrm{d}\omega_s \mathrm{d}\omega_i |f(\omega_s, \omega_i)|^2}.$$

(3)

For a separable input biphoton state with factorable joint spectral amplitude $|\psi_s\rangle \otimes |\psi_i\rangle = \iint \mathrm{d}\omega_s \mathrm{d}\omega_i f_1(\omega_s) f_2(\omega_i) \hat{a}_s^\dagger(\omega_s) \hat{a}_i^\dagger(\omega_i) |0\rangle$ we find

$$p(\tau) = \frac{1}{2} - \frac{1}{2} \frac{\left| \int \mathrm{d}\omega f_1^*(\omega) f_2(\omega) e^{-\imath \tau \omega} \right|^2}{\int \mathrm{d}\omega |f_1(\omega)|^2 \int \mathrm{d}\omega |f_2(\omega)|^2},$$

(4)

where positivity of the fraction term ensures $p(\tau) < 0.5$. We conclude that $p_c > 0.5$ implies a nonseparable, i.e., entangled two-photon input state

$$p(\tau) > 0.5 \Rightarrow |\psi_{s,i}\rangle \neq |\psi_s\rangle \otimes |\psi_i\rangle.$$

(5)

Thus the HOM coincidence detection probability $p(\tau)$ serves as a witness of entanglement in analogy to the polarization Bell-state analyzer. We note that additional entanglement in other degrees of freedom will not invalidate this relation. In addition we would like to stress that in contrast to entanglement detection in other degrees of freedom, e.g., polarization or transverse momenta, the presence of broadband frequency mode entanglement in a biphoton with amplitude $f(\omega_s, \omega_i) = u_0(\omega_s) u_1(\omega_i) - u_1(\omega_s) u_0(\omega_i)$ leads to a beating signature in $p(\tau)$ in general, whereas all other types will just switch between Gaussian dip and "bump" shape.

In the experiment as shown in Fig. 2, we employ a
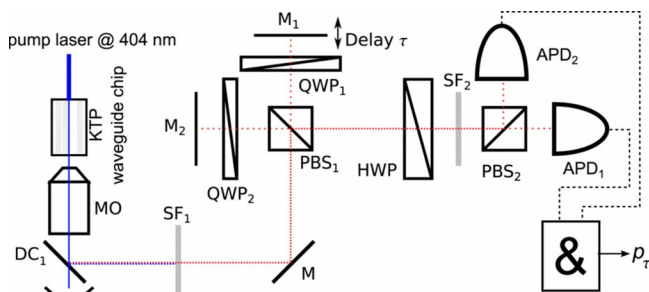
periodically poled KTP waveguide with dimensions $12\ \mathrm{mm} \times 4\ \mu\mathrm{m} \times 4\ \mu\mathrm{m}$, which is pumped by a picosecond diode laser at 404 nm with 1.4 nm FWHM and a repetition rate of 16 MHz. We excite a type II PDC process with orthogonally polarized signal and idler photons and central frequencies around 808 nm. After the signal and idler photons are split at PBS_1, we utilize a Michelson-type interferometer configuration with two additional quarter-wave plates QWP_1 and QWP_2 to introduce a variable delay between the orthogonally polarized photons. A spectral filter SF_1 centered around 808 nm with 3 nm FWHM is introduced to enhance signal-to-noise ratio. We then enter a common path HOM interferometer of the first type [18]; the half-wave plate HWP and PBS_2 act as a balanced beam splitter on both incoming polarization modes, where the HOM interference takes place. Subsequently, the output photons are detected with a pair of avalanche photodiodes (APDs), and coincident photons impinging on the detectors are counted separately. Single-photon event-count rates are of the order of 100 kHz or 1/160 events per pump pulse, thus justifying the neglect of multiple photon pair creation during one pump pulse.

Our measurement results are given in Fig. 3(c). We observe a beating signature in the coincidence probability $p(\tau)$, which can be seen as the sum of a bump signature and a wider dip signature. It is in good agreement with the assumption of broadband frequency mode entanglement in our PDC generated biphoton state; the overlap of the produced photon state with $|\psi^-\rangle$ is responsible for the central bump, the nonoverlapping rest for the dip. We note that in this simple picture, we have truncated our Hilbert space to include only the two lowest-order Hermite frequency modes. This result cannot be explained in terms of biphotonic output states of PDC in bulk crystals if the spectral pump envelope and phase-matching functions are modeled as Gaussian functions.

Typically the joint spectral amplitude $f(\omega_s, \omega_i)$ of a PDC output state $|\psi_{s,i}\rangle$ is calculated as a product of a spectral distribution of its pump envelope α and its phase-matching function Φ

Fig. 2. (Color online) Experimental setup.
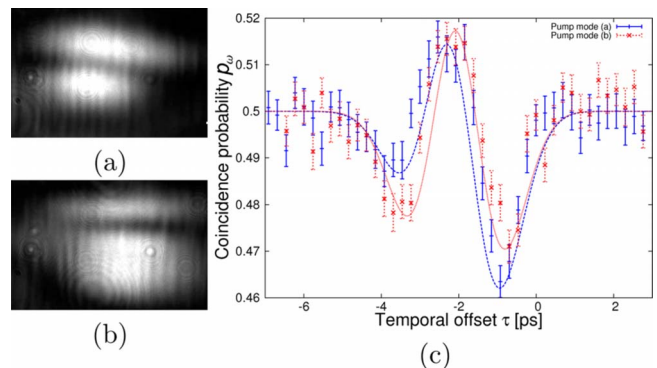
Fig. 3. (Color online) (c) Experimental results from two HOM measurements with (a),(b) different pump modes; visibility of theory curves (dashed curves) fitted to match observed visibilities.

$$\alpha(\omega_s + \omega_i) = e^{-(2\omega_c - \omega_s - \omega_i)^2/2\sigma^2}, \qquad (6)$$

$$\Phi(\omega_s, \omega_i) = \mathrm{sinc}\left(\frac{\Delta k L}{2}\right) e^{-\iota \Delta k L/2}, \qquad (7)$$

where Δk denotes the phase mismatch, L is the crystal length, and σ is the pump bandwidth. We assume the state to be frequency degenerate at ω_c, half the pump frequency. The phase-matching function Φ is simplified by applying a Gaussian approximation $\mathrm{sinc}(x) \approx e^{-\gamma x^2}$ with $\gamma = 0.193$.

To construct a joint spectrum in the PDC process, which exhibits a significant overlap with the broadband frequency entangled $|\psi^-\rangle$ state, we require a coherent superposition of two phase-matched PDC processes in the Gaussian approximation. Then the joint spectral amplitude shows two distinct maxima

$$f^{\pm}(\omega_s, \omega_i) = \alpha(\omega_s + \omega_i)\Phi\left(\omega_s \pm \frac{\Delta\omega}{2}, \quad \omega_i \mp \frac{\Delta\omega}{2}\right), \quad (8)$$

$$F(\omega_s, \omega_i) = f^+(\omega_s, \omega_i) + \mathrm{re}^{\iota\varphi} f^-(\omega_s, \omega_i). \qquad (9)$$

Equation (8) represents the spectral distributions symmetrically displaced from (ω_c, ω_c) by $\Delta\omega/\sqrt{2}$ as illustrated in Fig. 1(c). The spectral distribution of these superimposed PDC processes with a complex weighting factor $\mathrm{re}^{\iota\varphi}$ is given by Eq. (9). Comparing Fig. 1(b) with Fig. 1(c) already suggests that the overlap of the composite distribution F with the state $|\psi^-\rangle$ defined in Eq. (2) is nonnegligible, which is consistent with our calculations. The HOM interference probability between the signal and the idler of such a state evaluates to

$$p(\tau) = \frac{1}{2} - \frac{e^{-(\tau - \tau^-)^2/2\gamma\tau^{-2}}}{2\sqrt{C^+}}\frac{e^{-C^-/C^+} + \rho\cos(\Delta\omega\tau - \varphi)}{1 + e^{-C^-}\rho\cos(\Delta\omega\tau^- - \varphi)},$$

$$(10)$$

where we introduced the expressions $\tau^{\pm} = (\Delta k_s' \pm \Delta k_i') \times (L/2)$, $C^- = (\gamma/2)\Delta\omega^2(\tau^-)^2$, $C^+ = 1 + (\gamma/2)\sigma^2(\tau^+)^2$, $\rho = 2r/1 + r^2$, and $\Delta k_\mu = k_p'(2\omega_c) - k_\mu'(\omega_c)$ with $\mu \in \{s, i\}$.

The experimental data depicted in Fig. 3(c) matches our theoretical prediction of Eq. (10) closely for values of $\Delta\omega$ of 1.35 and 1.5 THz, respectively. The measurements differ in a slightly different alignment of the spatial pump modes [Figs. 3(a) and 3(b)], which was verified with a CCD camera monitoring the discarded pump beam. The reduced visibility of the experiments in comparison to the theory can be understood as a result of experimental imperfections, most prominently a non-Fourier-limited pump laser.

With the HOM fringes clearly visible, we can infer the existence of at least two distinct coherent spectral maxima of the PDC biphoton state, modeled by two Gaussian functions f^+ and f^- symmetrically displaced from (ω_c, ω_c). The sinc structure of the phase-matching function Φ, which we had simplified to be

Gaussian, might seem an obvious explanation for the spectral structure of our PDC process. However, calculations that use the parameters $\Delta\omega \approx 1.62$ THz, $\rho \approx 0.44$, $\varphi \approx (3/2)\pi$ to model the sinc characteristic, show that for our experimental situation the HOM interference results in a single dip shape. This leaves spatial waveguide mode triples [6], each with a slightly displaced phase-matching function due to modal dispersion, as the only possible explanation for our findings. This is also supported by different measurement outcomes for different pump modes.

In conclusion we have demonstrated that a waveguided PDC source is capable of producing broadband frequency-mode entangled photon pairs and that their entanglement affects HOMI experiments. Thus an HOMI signature serves as a witness of entanglement and allows us to ascertain a significant overlap of the PDC biphoton with the singlet Bell-state $|\psi^-\rangle$. While this effect surely has to be accounted for in integrated quantum networks using waveguides for state preparation, it also offers the possibility of information coding in the discrete frequency broadband modes for future communication protocols.

References

1. A. B. U'Ren, K. Banaszek, and I. A. Walmsley, Quantum Inf. Comput. **3**, 480 (2003).
2. L. A. Lugiato, A. Gatti, and E. Brambilla, J. Opt. B **4**, S176 (2002).
3. S. Tanzilli, H. de Riedmatten, W. Tittel, H. Zbinden, P. Baldi, M. de Micheli, D. B. Ostrowsky, and N. Gisin, Electron. Lett. **37**, 26 (2001).
4. M. E. Anderson, M. Beck, M. G. Raymer, and J. D. Bierlein, Opt. Lett. **20**, 620 (1995).
5. A. B. U'Ren, C. Silberhorn, K. Banaszek, and I. A. Walmsley, Phys. Rev. Lett. **93**, 093601 (2004).
6. K. Banaszek, A. B. U'Ren, and I. A. Walmsley, Opt. Lett. **26**, 1367 (2001).
7. S. Carrasco, J. P. Torres, L. Torner, A. Sergienko, B. E. A. Saleh, and M. C. Teich, Phys. Rev. A **70**, 043817 (2004).
8. C. K. Hong, Z. Y. Ou, and L. Mandel, Phys. Rev. Lett. **59**, 2044 (1987).
9. D. Branning, W. Grice, R. Erdmann, and I. A. Walmsley, Phys. Rev. A **62**, 013814 (2000).
10. M. Michler, K. Mattle, H. Weinfurter, and A. Zeilinger, Phys. Rev. A **53**, R1209 (1996).
11. M. Atatüre, A. V. Sergienko, B. E. A. Saleh, and M. C. Teich, Phys. Rev. Lett. **86**, 4013 (2001).
12. W. A. T. Nogueira, S. P. Walborn, S. Pádua, and C. H. Monken, Phys. Rev. Lett. **86**, 4009 (2001).
13. Z. Y. Ou and L. Mandel, Phys. Rev. Lett. **61**, 54 (1988).
14. J. G. Rarity and P. R. Tapster, Phys. Rev. A **41**, 5139 (1990).
15. H. Kim, J. Ko, and T. Kim, J. Opt. Soc. Am. B **20**, 760 (2003).
16. B. Dayan, Y. Bromberg, I. Afek, and Y. Silberberg, Phys. Rev. A **75**, 043804 (2007).
17. S. L. Braunstein and A. Mann, Phys. Rev. A **51**, R1727 (1995).
18. Y. H. S. Shih and A. V. Sergienko, Phys. Lett. A **191**, 201 (1994).